


Does upwelling intensity determine larval fish habitats in upwelling ecosystems? The case of Senegal and Mauritania

Maik Tiedemann¹  | Heino O. Fock¹ | Patrice Brehmer^{2,3} | Julian Döring⁴ | Christian Möllmann⁵

¹Federal Research Institute for Rural Areas, Forestry and Fisheries, Thünen Institute of Sea Fisheries, Hamburg, Germany

²Institut de Recherche pour le Développement (IRD), UMR 195 Lemar, Campus IRD-UCAD, Dakar, Sénégal

³Institut Sénégalais de recherche agricole (ISRA), Centre de Recherche Océanographique de Dakar-Thiaroye (CRODT), PRH, Dakar, Sénégal

⁴Leibniz Centre for Tropical Marine Research (ZMT), Bremen, Germany

⁵Institute for Hydrobiology and Fisheries Science, Center for Earth System Research and Sustainability (CEN), Klima Campus, University of Hamburg, Hamburg, Germany

Correspondence

Maik Tiedemann

Emails: maik.tiedemann@thuenen.de; tiedemann.maik@gmail.com

Funding information

German Federal Ministry of Education and Research (BMBF), Grant/Award Number: 01DG12073A (AWA); European Commission's Seventh Framework Programme, Grant/Award Number: 603521 (PREFACE); Institut de Recherche pour le Développement (IRD); Federal Research Institute for Rural Areas, Forestry and Fisheries, Thünen Institute of Sea Fisheries (TI-SF); Institute for Hydrobiology and Fisheries Science (IHF)

Abstract

European sardine (*Sardina pilchardus*) and round sardinella (*Sardinella aurita*) comprise two-thirds of total landings of small pelagic fishes in the Canary Current Eastern Boundary Ecosystem (CCEBE). Their spawning habitat is the continental shelf where upwelling is responsible for high productivity. While upwelling intensity is predicted to change through ocean warming, the effects of upwelling intensity on larval fish habitat expansion is not well understood. Larval habitat characteristics of both species were investigated during different upwelling intensity regimes. Three surveys were carried out to sample fish larvae during cold (permanent upwelling) and warm (low upwelling) seasons along the southern coastal upwelling area of the CCEBE (13°–22.5°N). *Sardina pilchardus* larvae were observed in areas of strong upwelling during both seasons. Larval habitat expansion was restricted from 22.5°N to 17.5°N during cold seasons and to 22.5°N during the warm season. *Sardinella aurita* larvae were observed from 13°N to 15°N during cold seasons and 16–21°N in the warm season under low upwelling conditions. Generalized additive models predicted upwelling intensity driven larval fish abundance patterns. Observations and modeling revealed species-specific spawning times and locations, that resulted in a niche partitioning allowing species' co-existence. Alterations in upwelling intensity may have drastic effects on the spawning behavior, larval survival, and probably recruitment success of a species. The results enable insights into the spawning behavior of major small pelagic fish species in the CCEBE. Understanding biological responses to physical variability are essential in managing marine resources under changing climate conditions.

KEYWORDS

Canary Current Large Marine Ecosystem, fish larvae, generalized additive models, Northwest Africa, *Sardina pilchardus*, *Sardinella aurita*, small pelagic fish, upwelling index

1 | INTRODUCTION

Alongshore trade winds induce a transport of surface water masses from the shelf break to the offshore in eastern boundary ecosystems. Consequently, nutrient-rich subsurface water is upwelled across the water column at the shelf break refilling the surface water

deficit and refueling primary production (Botsford, Lawrence, Dever, Hastings, & Largier, 2003; Ekman, 1905). In the Canary Current Eastern Boundary Ecosystem (CCEBE), the coastal upwelling is associated with the seasonal expansion of the intertropical convergence zone (ITCZ). In the cold season, in winter and spring, the ITCZ spreads along 6°N of the equator inducing a consistent band of

coastal upwelling at 12–35°N (Aristegui et al., 2009; Benazzouz et al., 2014). In the warm season in summer, the ITCZ expands northward (Doi, Tozuka, & Yamagata, 2009) and displaces the North Atlantic high poleward (Wooster, Bakun, & McLain, 1976) inducing permanent upwelling at 19–35°N (Figure 1). Meanwhile, trade winds at 12–19°N become replaced by monsoon winds starting in June (Benazzouz et al., 2014), whereas southeast trade winds from the South Atlantic high expand equatorward. Monsoon and southeast trade winds induce a decrease of wind speed and a change of wind direction from alongshore to onshore (Benazzouz et al., 2014; Doi et al., 2009). As a result, the coastal upwelling is reduced and fosters the northward advection of warm tropical surface water masses transported by the Mauritanian Current towards 12°–19°N of the CCEBE (Benazzouz et al., 2014; Cropper, Hanna, & Bigg, 2014; Mittelstaedt, 1991; Van Camp, Nykjaer, Mittelstaedt, & Schlittenhardt, 1991; Wooster et al., 1976).

The most dominant small pelagic fish species in the CCEBE are the European sardine (*Sardina pilchardus* Walbaum, 1792) and round sardinella (*Sardinella aurita* Valenciennes, 1847). Both species yield more than two-thirds of the total catches of small pelagic fishes from Morocco to the Gambia (Braham & Corten, 2015). *Sardina pilchardus* prefers the cold upwelled waters as a habitat for feeding and spawning (Ettahiri, Berraho, Vidy, Ramdani, & Do chi, 2003; ter Hofstede & Dickey-Collas, 2006; Machu et al., 2009). Spawning

takes place at optimally 16–18°C in Northwest Africa (Coombs et al., 2006). *Sardinella aurita*, however, prefers temperatures of 22–25°C for spawning (Conand, 1977). Thus, *S. aurita* reproduces in Guinean and southern Senegalese waters during the cold season in winter/spring and migrates with the summer influx of warm tropical water towards Mauritania and Morocco to spawn (Braham, Fréon, Laurec, Demarcq, & Bez, 2014; Zeeberg, Corten, Tjoe-Awie, Coca, & Hamady, 2008). Nevertheless, adults of both species occasionally co-exist locally sharing a similar diet composed of phyto-, zooplankton and detritus (Gushchin & Corten, 2015).

Cury and Roy (1989) observed a dome-shaped relationship between upwelling intensity and the recruitment success of fishes. They showed that a wind speed of 5 m s⁻¹ induces moderate upwelling intensity, but prevents strong turbulence which is detrimental to larval fish feeding success. At lower wind speeds, upwelling and thus primary production decrease reducing available food. At higher wind speeds, turbulence increases and hinders sufficient foraging as well as retention while deepening the mixed surface layer (Pollard, Rhines, & Thompson, 1973; Pringle, 2007). Thus, a pelagic fish is hypothesized to spawn in an optimal environmental window (OEW) by locally optimizing physical constraints (Cury & Roy, 1989). The OEW hypothesis is supported by recruitment studies of dominant small pelagic fish species like *S. pilchardus* in the northern part of the CCEBE (Roy, Cury, & Kifani, 1992), and also by

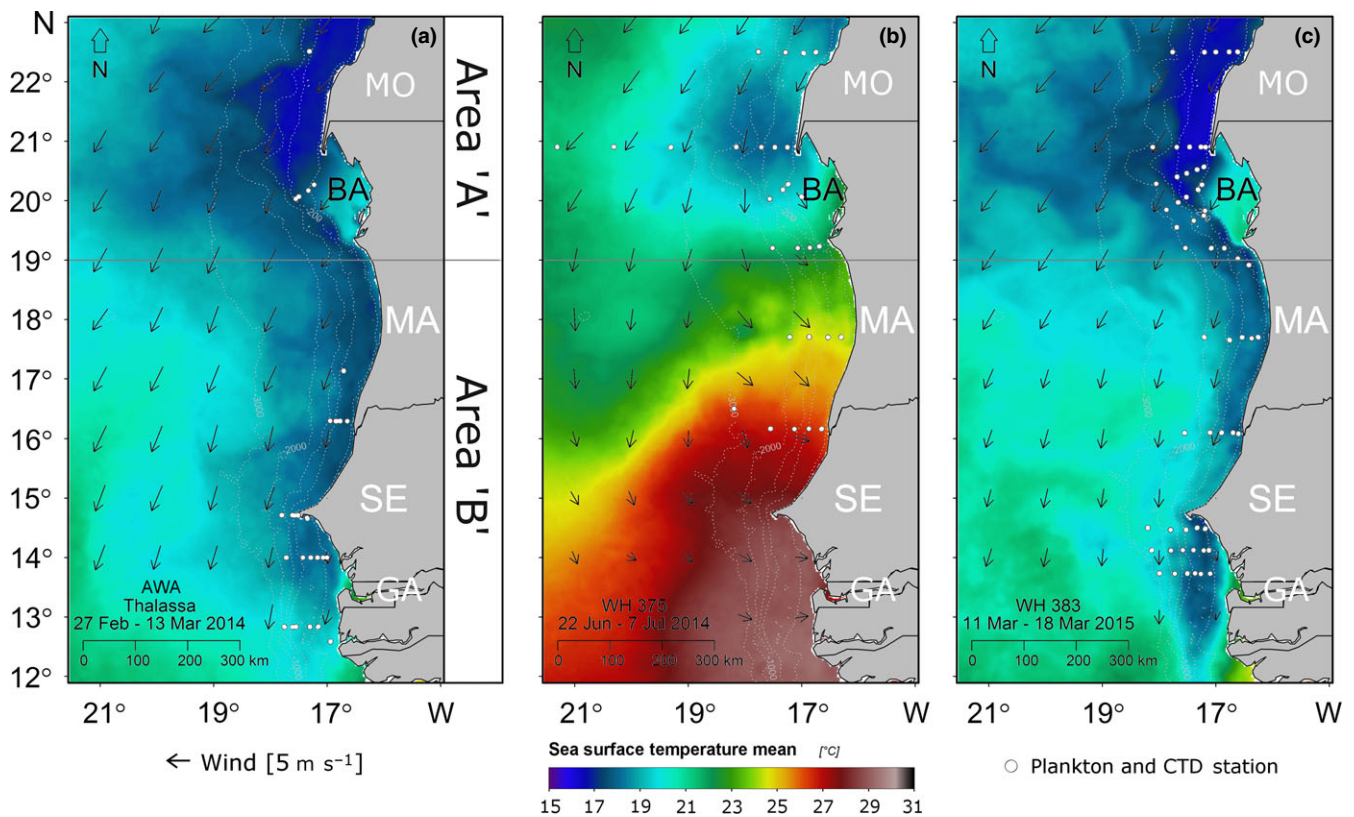


FIGURE 1 Sea surface temperature (JPLOurOceanProject, 2010) and surface wind regime (KNMI, 2010) derived from remote sensing and biological sampling stations (white dots) during the three surveys (a) cold season 2014 (b) warm season 2014 and (c) cold season 2015 along the southern part of the Canary Current Eastern Boundary Ecosystem, area is split into 'A', permanent upwelling area and 'B', seasonal upwelling area according to Cropper et al. (2014), MO, Morocco; BA, Banc d'Arguin; MA, Mauritania; SE, Senegal; GA, Gambia

species of all other major eastern boundary upwelling ecosystems: By the Southern African anchovy (*Engraulis capensis* Gilchrist, 1913) from the southern Benguela ecosystem (Waldron, Brundri, & Probyn, 1997), the Californian anchovy (*Engraulis mordax* Girard, 1854) from the California ecosystem (Cury et al., 1995; Roy et al., 1992) and the Chilean sardine (*Sardinops sagax* Jenyns, 1842) from the Humboldt ecosystem (Serra, Cury, & Roy, 1998).

Wind-induced upwelling intensity is predicted to increase as a result of elevated land-sea temperature differences driven by global warming (Bakun et al., 2015). A poleward displacement of upwelling-favorable winds is projected for the 21st century changing upwelling regimes in eastern boundary ecosystems (Rykaczewski et al., 2015). However, the upwelling process, which impacts timing and localization of fish spawning habitats, is not well understood.

The aim of the present study was to identify larval habitats of *S. pilchardus* and *S. aurita* in either, the permanent upwelling during the cold season, or in the reduced upwelling in the warm season. It is the first attempt to attribute upwelling conditions in the southern part of the CCEBE to larval fish distribution patterns and whether the upwelling intensity may regulate the larval occurrence of *S. pilchardus* and *S. aurita*. For this purpose, we sampled the seasonal upwelling area and the southern part of the permanent upwelling area of the CCEBE (Cropper et al., 2014) for one seasonal cycle. Because of anticipated changes in upwelling intensity, owing to climate warming, understanding the main drivers of spawning time and area is the key in predicting possible impacts on the CCEBE small pelagic resources. With our observations, we addressed two hypotheses to indicate (i) whether the seasonality in upwelling intensity may trigger the occurrence of either *S. pilchardus* larvae in the cold season or *S. aurita* larvae in the warm season due to adult spawning preferences; and (ii) whether asynchronous spawning leads to a spatio-temporal niche partitioning between the larvae of both species.

2 | MATERIALS AND METHODS

2.1 | Survey design

We explored these hypotheses using data collected by three sea-going surveys (Table 1) using the same device and methodology to collect fish larvae at 112 stations along 22.5°N–12.5°N latitude (Figure 1). On each survey, plankton samples were taken with a modified GULF VII plankton net (0.03 m² mouth and 280 μm mesh, No. 438 410; Hydro-Bios, Kiel, Germany). Double oblique hauls were conducted sampling the water column from surface to 5 m above

the sea floor or a maximum depth of 200 m at deeper stations. Sampling took place at day ($N = 61$), night ($N = 45$) and twilight ($N = 6$). Quadruple oblique hauls ($N = 16$) were conducted at stations with 20–30 m bottom depth to filter at least 20 m³ of water. The mean ship speed was 5 knots veering and heaving the net with 0.7 m/s. A conductivity-temperature-depth (CTD) probe with two electronic flow meters (No. 450 100; Hydro-Bios, Kiel, Germany) attached to the GULF VII measured *in-situ* depth [m], temperature [°C], salinity and filtered water volume [m³/s]. Additional CTD casts using a Sea-bird 911plus profiler (Sea-Bird Electronics Inc., Bellevue, WA, USA) were used to validate temperature and salinity measurements.

Samples were fixed immediately after the haul using a 4% formalin and freshwater solution buffered with borax. After a minimum fixation time of 24 h the formalin fixative was replaced by a non-toxic sorting fluid (0.5% propylene phenoxetol, 4.5% propylene glycol and 95% freshwater). Larvae of *S. pilchardus* and *S. aurita* were sorted out, and their densities [ind m⁻³] were standardized to an abundance index [ind 10⁻¹ m⁻³] (Smith & Richardson, 1977). Ontogenetic stages were classified according to pre-, flexion and postflexion for *S. pilchardus* (Ré & Meneses, 2008; Russell, 1976) and *S. aurita* (Conand, 1978; Ditty, Houde, & Shaw, 1994).

2.2 | Coastal upwelling index (CUI_{SST})

A measure of the upwelling intensity was derived from sea surface temperature (SST) that was based on remote sensing data (JPLOurOceanProject, 2010) to investigate the influence of upwelling intensity on the occurrence of *S. pilchardus* and *S. aurita* larvae (Benazzouz et al., 2014). While calculating the coastal SST minimum (SST_{min}) of a certain latitude and subjecting a maximum SST (SST_{max}) from an arbitrarily set point in the open ocean on the same latitude, the thermal contrast is depicted by the coastal upwelling index CUI_{SST} (Mittelstaedt, 1991; Roy et al., 1992; Santos, de Fátima Borges, & Groom, 2001; Van Camp et al., 1991). A CUI_{SST} was derived by the thermal contrast between the SST_{min} from the continental shelf area and the SST_{max} from the entire mid Atlantic Ocean (Benazzouz et al., 2014):

$$\text{CUI}_{\text{SST}}(\text{lat, time}) = \text{SST}_{\text{max offshore}(\text{lat, time})} - \text{SST}_{\text{min inshore}(\text{lat, time})} \quad (1)$$

SST data were extracted from daily SST products using the Sea-DAS software version 7.2 (<http://seadas.gsfc.nasa.gov/>). SST products were averaged to the survey periods to receive a high coverage of SST data in spite of cloud cover. SST data were extracted from pixel data based on 0.01° × 0.01° grids. The minimum SST (SST_{min}) was derived from the coastline to 18°W to include the area of the

TABLE 1 Survey dates and number (n) of GULF samples in the southern part of the Canary Current Eastern Boundary Ecosystem

Cruise	Project	Vessel	Date	Year	Season	Samples (n)
AWA	AWA/PREFACE	FRV Thalassa	27 Feb–13 Mar	2014	Cold (Winter/Spring)	28
WH 375	AWA/PREFACE	FRV Walther Herwig III	22 Jun–7 Jul	2014	Warm (Summer)	28
WH 383	AWA/PREFACE	FRV Walther Herwig III	11 Mar–18 Mar	2015	Cold (Winter/Spring)	56

coastal upwelling at the continental shelf break. Maximum SST (SST_{max}) was obtained from the coast and 45°W corresponding to the mid-Atlantic Ocean. The CUI_{sst} was acquired for each survey period to describe the upwelling phenomenon along the whole sampling area. Additionally, the CUI_{sst} of each sampling station was derived from SST_{min} and SST_{max} of each sampling station latitude. CUI_{sst} of each station was used as an explanatory variable in generalized additive models (GAMs) to elucidate the impact of different upwelling intensities on spatially based larval fish abundances (LFAs).

2.3 | Wind speed and direction

Wind speed and direction were obtained from coastal ocean surface wind vector retrievals and projected to $1^\circ \times 1^\circ$ grids (KNMI, 2010). Both were projected to highlight upwelling favorable wind fields during the cold season surveys and the additional southeast trade winds during the warm season survey. Wind patterns are included in Figure 1 and a more detailed figure of wind rose plots are attached in the supplement (Figure S1). For comparability reasons, we defined two study areas, a permanent ('A') and a seasonal ('B') upwelling area (Cropper et al., 2014). The permanent upwelling area 'A' comprised the southern Morocco and the Banc d'Arguin coastal area (19–23°N latitude) and the seasonal upwelling area 'B' comprised the southern Mauritanian and Senegalese coastal area (12–19°N latitude). To compare the environmental differences between the two areas and cold and warm season conditions, we used the Welch *t* test for unequal sample numbers and unequal variances on mean values of CUI_{sst} , wind speed, in-situ salinity and sea surface temperature (Welch, 1951).

2.4 | Linking environmental data with larval fish abundance

GAMs were used to investigate the influence of environmental factors on larval *S. pilchardus* and *S. aurita* abundance data (Roy, Cury, Fréon, & Demarcq, 2002) using the 'mgcv' package within the R software version 3.2.2 (Wood, 2006). GAMs extend general linear models allowing for complex correlations between response and explanatory variables (Hastie & Tibshirani, 1986), but subject to the same prerequisites (Zuur, Ieno, & Elphick, 2010).

Thus, multi-collinearity of explanatory variables was tested *a-priori* using the variance inflation factor (VIF) on latitude (Lat), longitude (Long), temperature at 5 m depth [°C] (SST), salinity at 20 m depth (SAL), bottom depth [m] and CUI_{sst} [°C] (Crane & Surles, 2002). The VIF quantitates multi-collinearity by providing an index of how much the variance of an estimated regression coefficient increases because of collinearity of predictor variables (Murray, Nguyen, Lee, Remmenga, & Smith, 2012). Salinity at 20 m depth was used because the salinity profiles were most stable at 20 m depth and only small changes were observed from surface salinity values and values at 20 m depth during CTD casts. Multi-collinearity testing revealed a correlation between SST and CUI_{sst} (VIF = 8.6). Using a more stringent approach either CUI_{sst} or SST was removed

in the GAMs. After the removal, a VIF < 3 for all tested explanatory variables was considered adequate (Zuur et al., 2010). Spatial autocorrelation was tested by investigating residuals from the final GAM with Moran's I within the R package 'ape' (Gittleman & Kot, 1990) resulting in non-significant *p*-values for both species (*p* > .05). A Tweedie distribution assumption was used to resolve the issue of zero-inflation (Augustin, Trenkel, Wood, & Lorange, 2013; Shono, 2008) typical when dealing with count data (Fahrig, 1992; Mcgurk, 1986) and was compared to model outputs with Poisson, negative binomial and zero-inflated Poisson distribution assumptions. The Tweedie distribution is a flexible Poisson – Gamma distribution assumption, whereas the dispersion parameter *p* = 1 depicts a Poisson distribution and *p* = 2 a Gamma distribution. Dispersion parameter was set to 1.4 based on an estimated parameter during final GAM fitting.

The final GAM construction for larval *S. pilchardus* abundance data (y_i) followed the equation:

$$E(y_i) = g^{-1}[\beta_0 + \text{season}_i + f_1(\text{lat}_i, \text{long}_i) + f_2(CUI_i)] + \varepsilon \quad (2)$$

and for larval *S. aurita* abundance data (y_i) the equation:

$$E(y_i) = g^{-1}[\beta_0 + \text{season}_i + f_1(\text{lat}_i, \text{long}_i) + f_2(CUI_i) + f_3(SAL_i) + f_4(\text{bottom depth}_i)] + \varepsilon \quad (3)$$

where $E(y_i)$ equals expected values of either *S. pilchardus* or *S. aurita* abundance based on a Poisson, negative binomial or Tweedie distribution where g^{-1} denotes a log-link function, or a zero-inflated Poisson distribution with an identity-link function. β_0 equals the intercept and ε the residual error that cannot be predicted from knowledge of the predictors. LFA data were adjusted to non-negative integer values to satisfy distribution assumptions for count data (Rooper et al., 2012). We used season_i as categorical variable for cold and warm season. Smoothing parameters with tensor product smoother (f_1) for location 'longitude and latitude' (Augustin et al., 2013) and panelized thin plate regression splines (f_{2-4}) for other input variables were estimated by the Restricted Maximum Likelihood for negative binomial, zero-inflated Poisson and Tweedie or the Unbiased Risk Estimation for Poisson distribution assumption. Thin plate regression splines are considered an ideal smoother of any predefined dimension (Wood, 2003). A spline curve consists of piecewise polynomial curves joining two or more polynomial curves. The joint locations are known as 'knots' (Wood, 2006). The number of knots was limited to *k* = 3 for the smoother SST, SAL, bottom depth and CUI_{sst} to avoid overfitting of the model (Alvarez-Berastegui et al., 2016).

Model selection was based on a manual backward stepwise procedure including the evaluation of (i) model performance significance testing (*p* < .05), (ii) the Akaike information criterion (AIC) and (iii) residual plots for 'independency', 'homogeneity' and 'normality' of residuals (Wood, 2006; Zuur et al., 2010). After model selection, each explanatory variable was stepwisely excluded from the final model to examine the change in deviance explained providing a means of importance for each variable (Rooper et al., 2012). Additionally, generalized additive mixed models (GAMMs), which were

based on the previous GAM set-up, were used to correct for spatial autocorrelation not only in the covariates (Augustin et al., 2013; Winton, Wuenschel, & McBride, 2014), but also in the error term ε_i (Beale, Lennon, Yearsley, Brewer, & Elston, 2010; Wood, 2006). GAMMs were used to investigate a possible improvement of the previous GAMs.

The best models according to formula (2) and (3) were used to predict larval fish habitats in both seasons. The aim was to verify final models and to map predictions on a spatial grid. For this, we used the predict function of the 'mgcv' package in R version 3.2.2. We expanded the predictions on a $0.1^\circ \times 0.1^\circ$ grid of the sampling area. An ordinary kriging procedure provided by the 'gstat' package in R was used to plot cold and warm season predictions (Pebesma, 2004).

3 | RESULTS

3.1 | Environmental conditions

General environmental conditions during both cold season surveys appeared similar and were typical for the survey periods. In both surveys, northeasterly trade winds induced an upwelling of cold subsurface water along the continental shelf over the study area (Figure 1a and c). In both years, northeasterly trade winds of 7–8 m/s likely stimulated upwelling and pushed the upwelling front offshore to the 2,000-m isobath in area 'B'. In area 'A', higher wind speeds of 8–10 m/s (Welch's t test, $p < .05$) transported upwelled water even further offshore. This observation was in line with slightly stronger upwelling in area 'A' with CUI_{SST} values of 6.6–6.9°C than in area 'B' with CUI_{SST} values of 6.4–6.7°C (Welch's t test, $p < .05$) (Figure 2). Minimum coastal SST that represents the newly upwelled subsurface water increased from 16.8°C in area 'A' to 18°C in area 'B' (Welch's t test, $p < .05$). Salinity decreased from 36.4 to 35.8 from area 'A' to 'B' (Welch's t test, $p < .05$) indicating two water masses that are delimited at the Cape Verde Frontal Zone (Zenk, Klein, & Schroder, 1991). This frontal zone splits North Atlantic central water masses in the North of area 'A' with South Atlantic central water masses originating from the south of the study area (Pastor et al., 2008; Tomczak, 1981).

A contrasted situation in the 2014 warm season survey is characterized by an influx of warm surface water off area 'B'. The influx of warm water is fostered by the Mauritania Current transporting warm surface waters from the Guinea Dome poleward (Faye, Lazar, Sow, & Gaye, 2015). A fraction of prevailing northwesterly monsoon winds (6 m s^{-1}) perpendicular to the coast was apparently too weak to induce coastal upwelling. Off area 'A' northeasterly trade winds (8 m s^{-1}) dominated inducing an upwelling of cold subsurface waters and transporting the cold waters at the surface across the 2,000m isobath offshore. Here, the permanent upwelling revealed a mean CUI_{SST} of 6.7°C similar to the cold season conditions in both cold season surveys. This area is the southern limit of the permanent upwelling in the CCEBE (Cropper et al., 2014). Further south of the study area the upwelling intensity decreased significantly to a CUI_{SST}

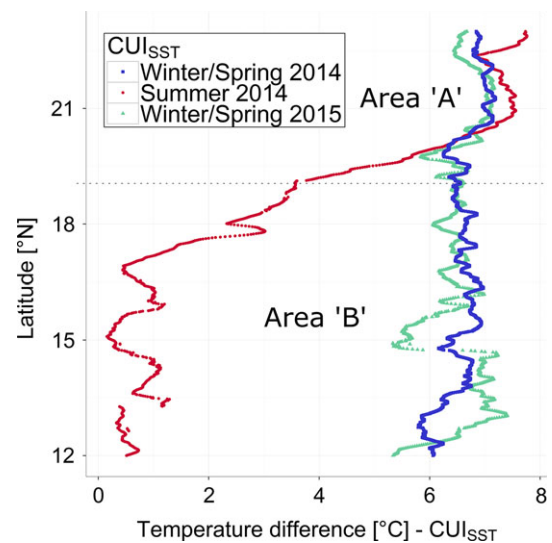


FIGURE 2 Latitudinal-based coastal upwelling index (CUI_{SST}) along 21.5–12°N for the three surveys (Table 1), blue and green dots display cold season indicating upwelling, red dots indicate warm season with upwelling in the permanent upwelling area at 21.5–19°N and reduced upwelling in the seasonal upwelling area at 19°N–12°N, dashed line indicate the boundary between area 'A' (permanent upwelling area) and area 'B' (seasonal upwelling area). [Colour figure can be viewed at wileyonlinelibrary.com]

of 1.3°C (Welch's t test, $p < .05$) in area 'B'. We exclusively recorded positive CUI_{SST} values indicating that area 'B' was still influenced by persistently upwelled subsurface water. While the minimum coastal SST increased from 19°C to 26°C, salinity decreased from 36.6 to 35.8 from area 'A' to 'B' again indicating the separation of North Atlantic central water and South Atlantic central water at the Cape Verde Frontal Zone. For detailed seasonality of hydrography in the CCEBE see Faye et al. (2015).

3.2 | Horizontal larval fish distribution patterns: Observation, model selection and validation

In total, we collected 1,755 *S. pilchardus* and 2,841 *S. aurita* larval specimens. *S. pilchardus* was mainly present in the cold season surveys and only present in coastal upwelling waters. *S. aurita* larvae mostly occurred during the warm season. Besides the temporal partitioning, *S. pilchardus* was found in the northern part of the study area southward to 17.5°N (Figure 3). *S. aurita* occasionally occurred off Senegal in the cold season and with high abundances from 16°N to 21°N along the Mauritanian coast in the warm season. No spatiotemporal co-occurrence of both species could be observed indicating a larval niche partitioning.

3.3 | *Sardina pilchardus*

Maximum larval *S. pilchardus* abundances of 10,400 ind 10^{-1} m^{-2} were observed close to the coast in the northernmost transect decreasing towards offshore in the cold season surveys (Figure 3). High larval fish abundances (LFAs) were also observed in area 'A' in

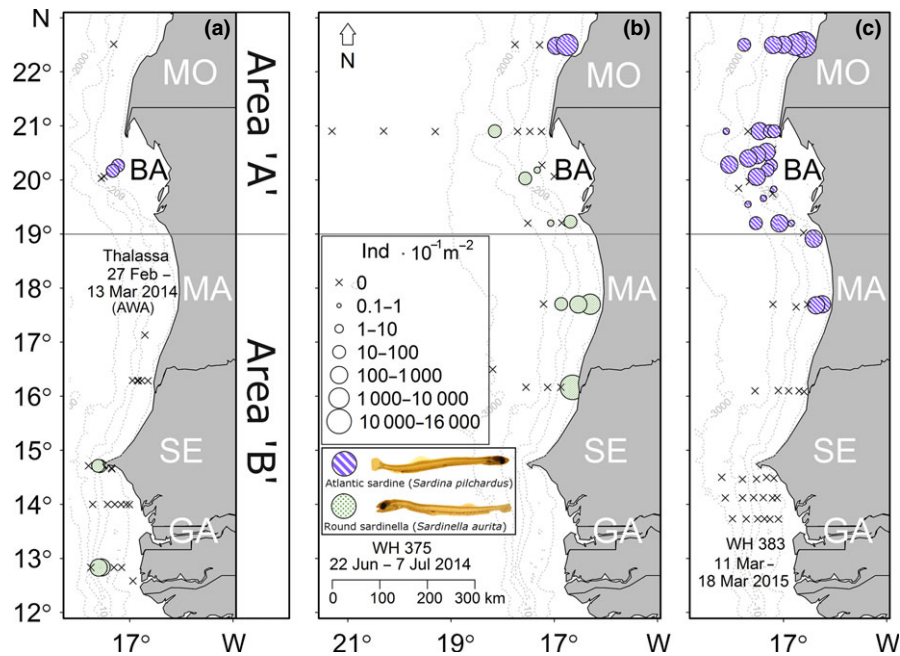


FIGURE 3 Distribution and larval fish abundance patterns of European sardine (*Sardina pilchardus*) and round sardinella (*Sardinella aurita*) during the three surveys (a, c) cold season and (b) warm season along the southern part of the Canary Current Eastern Boundary Ecosystem, area is split into area 'A', permanent upwelling area and 'B', seasonal upwelling area according to Cropper et al. (2014), MO, Morocco; BA, Banc d'Arguin; MA, Mauritania; SE, Senegal; GA, Gambia

2015 cold season with some specimens found in the northernmost part of area 'B' southward to 17.5°N. Larvae were absent further south, similar to the 2014 cold season survey where only some specimens were collected at stations of the Banc d'Arguin transect. In the 2014 warm season survey, larval distribution was restricted to the permanent upwelling in the northernmost transect. Larvae occurred mainly on the continental shelf (primarily between 50 and 200 m bottom depth) and occasionally with lower abundances at stations as far as 2,000m bottom depth. Higher proportions of preflexion larvae (82% shelf versus 69% offshore) indicated a transport offshore within the upwelling frontal zone. In total, the ontogenetic characterization resulted in the proportion of 81% preflexion, 16% flexion and 3% postflexion. Larvae were only collected in the strong upwelling ($CUI_{sst} > 6^{\circ}C$) in both seasons.

The best-fit GAM accounted for 92% explained deviance (Table 2). Significant partial effects of location (latitude and longitude) explained 72%, CUI_{sst} 19%, and season 1% of the deviance. The partial effects are presented as best-fit smooth plots in Figure 4 and predictions of the best-fit GAM are shown in Figure 6. The smooth plot of 'location' indicated an increasingly higher probability of larval occurrences the closer to the coast and the further to the north of the sampling area. A positive linear correlation between LFA and CUI_{sst} indicated increasing probability of larval occurrences with increasing CUI_{sst} . Both partial effects suggest a larval habitat along the permanent upwelling consistent with field observations. The smooth plot of the factor 'season' revealed significantly higher LFAs in the cold seasons than in the warm season. Given a low probability of LFA during the warm season, the partial effect 'season' indicated a subsidiary period of *S. pilchardus* spawning in the

southern CCEBE. Larval habitat maps predicted by the best-fit GAM were consistent with habitat preferences in the permanent upwelling regime of the northern part of the study area (Figure 6).

The underlying quantile-quantile plot and histogram of residuals of the best-fit GAM indicated no issues with normality (Figure S2). Homogeneity plots were skewed due to the many zero counts but fitted best compared to all other tested models. Similar results were produced by the GAMMs, but no improvement compared to the GAM output could be observed. The negative binomial assumption was the only assumption, which similarly fitted well in the GAMs like the Tweedie distribution assumption, but resulted in lower deviance explained and poorer residual plots (Table 2). Poisson and zero-inflated assumptions resulted in ecologically unrealistic responses providing infinite significant effects of all 'partial effects' during fitting.

3.4 | *Sardinella aurita*

Sardinella aurita larvae were most abundant during the warm season with maximum abundances of $15,400 \text{ ind} \cdot 10^{-1} \text{ m}^{-2}$ at the southernmost coastal station (Figure 3). Larval distribution patterns revealed occurrences in the area with warm tropical water influx indicating spawning in the reduced upwelling along the continental shelf. Highest abundances could be noted in the Senegalese and Mauritanian coastal area with decreasing abundances towards the Banc d'Arguin. No larvae were found further north in the study area indicating suspended spawning in the upwelling area. Only a few specimens occurred in the southern Senegalese coastal area during the cold season survey 2014. In the cold season survey 2015, no

TABLE 2 Results of generalized additive models (GAM) and mixed models (GAMM) based on larval European sardine (*Sardina pilchardus*) and round sardinella (*Sardinella aurita*) abundance data on explanatory variables (Season, Lat, latitude and Long, longitude; SAL, salinity; CUI_{sst}, coastal upwelling index, bottom depth), different family distribution assumptions (P, Poisson; NB, negative binomial; ZIP, zero-inflated Poisson; T, Tweedie); n/a, not available; Dev. expl., deviance explained [%]; MCNA, model convergence not achieved; Signif. codes: <000.1 '***' 0.001 '**' 0.01 '*' 0.05. NS, not significant

Species	Model	Family	Season	Lat, Long	SAL	CUI _{sst}	Bottom depth	Dev. expl.
<i>Sardina pilchardus</i>	GAM	P	Overfitted					
		NB	***	***	NS	NS	NS	89.5
		ZIP	Overfitted					
		T	***	***	NS	*	NS	92.1
	GAMM	P	***	***	NS	**	*	n/a
		NB	MCNA					
		ZIP	n/a					
		T	***	***	NS	**	*	n/a
<i>Sardinella aurita</i>	GAM	P	Overfitted					
		NB	*	***	***	***	***	96.0
		ZIP	Overfitted					
		T	*	***	***	***	***	97.6
	GAMM	P	MCNA					
		NB	MCNA					
		ZIP	n/a					
		T	MCNA					

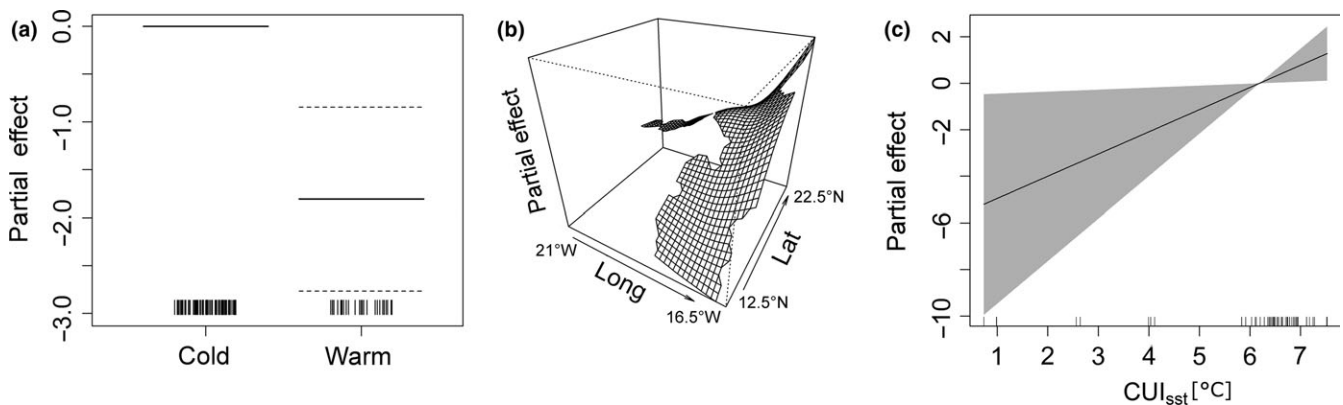


FIGURE 4 Partial effects of generalized additive model output for European sardine (*Sardina pilchardus*) larval fish abundance data based on a Tweedie distribution assumption, (a) Season, (b) Location (Lat, latitude; Long, longitude) and (c) Coastal upwelling index (CUI_{sst}), gray area represents 95% confidence interval

larvae were observed. At 20.9°N latitude during the 2014 summer cruise, some specimens were collected at 2,000 m isobaths. 92% of the sampled preflexion larvae occurred on the shelf and 29% offshore indicating a larval transport offshore. The ontogenetic characterization revealed that in total 88% were in the preflexion, 4% in the flexion and 8% in postflexion.

The best-fit GAM accounted for 97.6% explained deviance. Significant partial effects of CUI_{sst} explained 59.2%, salinity 25.7%, location (latitude and longitude) 9.4%, bottom depth 3.8% and season <0.1% (Figure 5). A negative linear correlation between LFA and CUI_{sst} indicated decreasing probability of larval fish occurrences with increasing CUI_{sst}. Larval occurrences were associated with water

masses of salinities between 35.6 and 36.2. Larvae were absent in higher salinity water masses indicating spawning in South Atlantic central waters. The smooth plot of location revealed an increasing probability of high LFAs from north to south. A negative linear correlation between LFA and bottom depth indicated increasing probability of LFA with decreasing bottom depth. Model outputs revealed larval habitats that were associated with the shelf and the shelf break until approximately 1,000m bottom depth. The partial effect of CUI_{sst} explained 15% more than the also significant partial effect SST and was used in the best-fit GAM for *S. aurita*. Larval habitat map, predicted by the best-fit GAM, were consistent with habitat preferences in the waters masses of the tropical influx during the

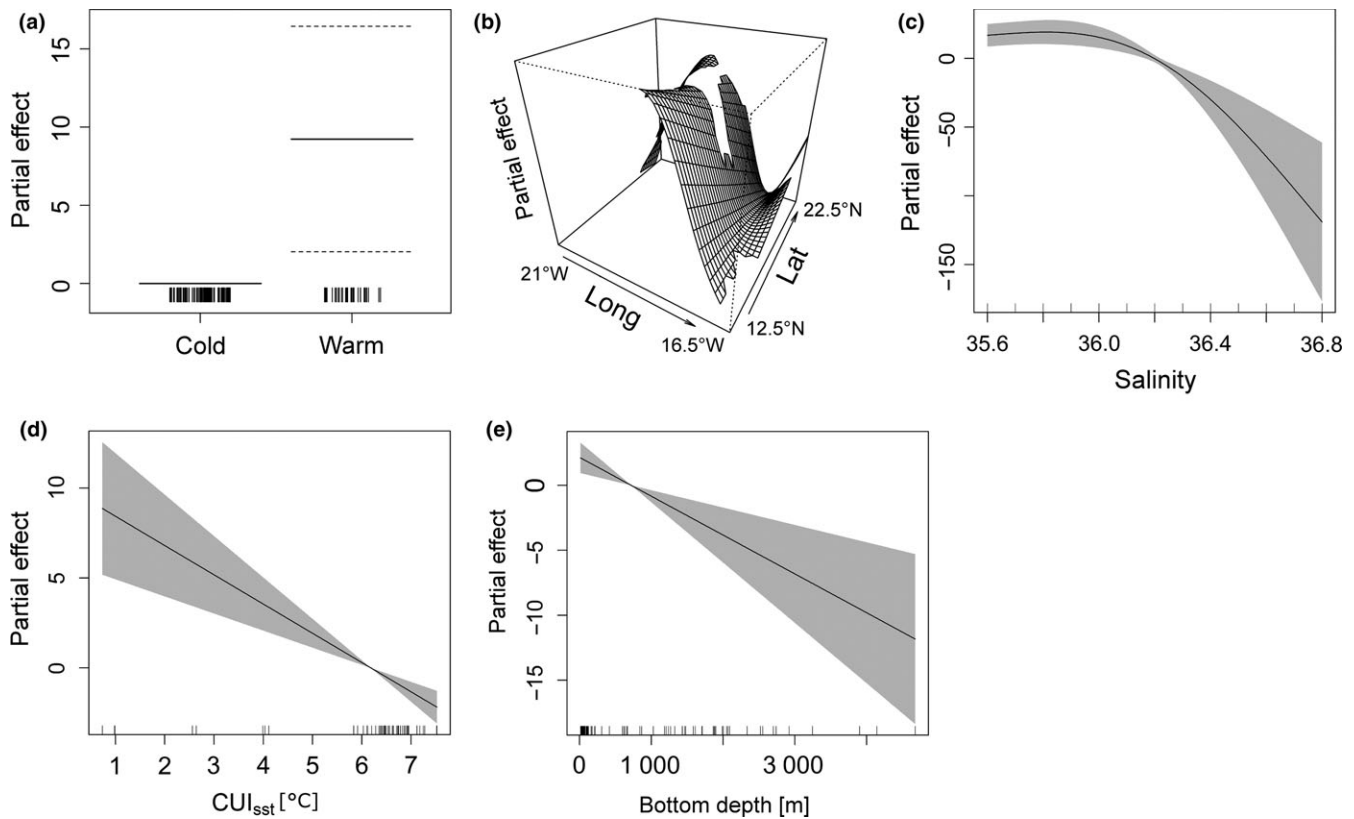


FIGURE 5 Partial effects of generalized additive model output for round sardinella (*Sardinella aurita*) larval fish abundance data based on a Tweedie distribution assumption. (a) Season, (b) Location (Lat, latitude; Long, longitude), (c) Salinity, (d) Coastal upwelling index (CUI_{sst}) and (e) Bottom depth, gray area represents 95% confidence interval

warm season (Figure 6). In the cold season, larval habitats were associated with the upwelling core off the southern Senegalese region.

The comparison of the different distribution assumptions during GAM computation revealed either overfitting, except for Tweedie or negative Binomial, or no achievable convergence in GAMM computation (Table 2). Negative binomial resulted in 1.6% less deviance explained than Tweedie, and residual plots were stronger skewed than the residual plot of the Tweedie distribution assumption (Figure S3). Considering 90% zero observations of *S. aurita* LFA, the Tweedie distribution still produced reliable outputs.

4 | DISCUSSION

The decrease in upwelling intensity from the cold to the warm season revealed two contrasting larval habitats of *S. pilchardus* and *S. aurita* in the seasonal upwelling area of the CCEBE. While the permanent upwelling in area 'A' seemingly shaped a favorable habitat for *S. pilchardus* reproduction, *S. aurita* reproduced mainly in the warm season during periods, when the SST contrast between offshore waters and the coast was small (low CUI_{sst}) which was driven by the influx of warm, tropical, surface water. The shift in upwelling intensity revealed self-contained larval *S. pilchardus* and *S. aurita* distribution areas. Observation as well as modeling were consistent

with our hypothesis of asynchronous spawning behavior, which led to a spatio-temporal niche partitioning in larval fish abundances.

Niche partitioning is based on the concept that organisms out-compete competitors by diminishing resources below a competitor's survival threshold leading to a diversification in habitat choice (Schoener, 1974). Habitat choice is based on seasonality in the tropical ocean due to annually changing hydrographical features that control species' spawning times (Johannes, 1978; León-Chávez, Beier, Sánchez-Velasco, Barton, & Godínez, 2015). Adjusted successive spawning in clupeid fishes might have evolved to avoid competition by eliminating resource differentiation that would emerge from larval co-occurrence (Wang & Tzeng, 1997). Adults of *S. pilchardus* and *S. aurita* occasionally co-occur in the seasonal CCEBE upwelling area (Gushchin & Corten, 2015; ter Hofstede & Dickey-Collas, 2006). Thus, adult co-occurrences might indicate stronger competition for space and food than during respective species' larval development phases. This leaves the conclusion that niches are differently occupied during the life history of fishes (Tsikliras, 2014).

However, the present observations represent 1 year of data and the full extent of the stocks of interest are not entirely covered on a seasonal and spatial basis. Both, *S. pilchardus* and *S. aurita* spawning areas, have been reported north of the present study location with eggs of the southern stock of *S. pilchardus* extending at least to 26°N (Machu et al., 2009) and *S. aurita* to at least 24°N (Ettahiri et al., 2003) with some larval spatio-temporal co-occurrences.

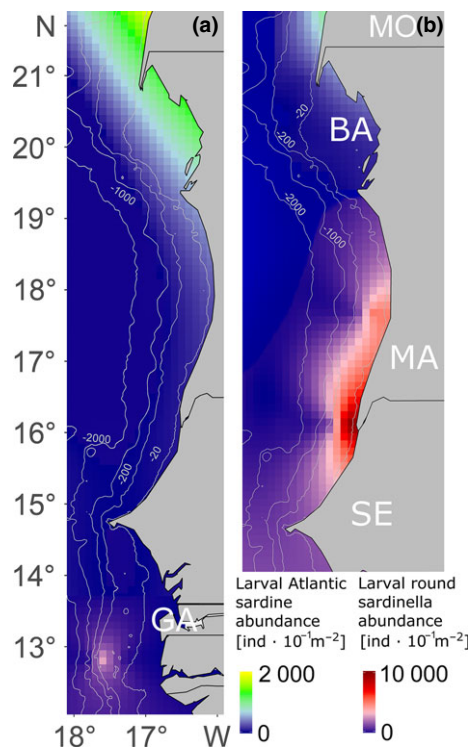


FIGURE 6 Cold season “winter/spring” (a) and warm season “summer” (b) larval fish abundance predictions of European sardine (*Sardina pilchardus*, green) and round sardinella (*Sardinella aurita*, red) based on generalized additive model output, MO, Morocco; BA, Banc d’Arguin; MA, Mauritania; SE, Senegal; GA, Gambia

Studies from other eastern boundary ecosystems that have decades of data, illustrate relationships between upwelling intensity and larval distributions, but are susceptible to change over time (Lluch-Belda, Lluch-Cota, Hernandez-Vazquez, Salinas-Zavala, & Schwartzlose, 1991; Mhlongo, Yemane, Hendricks, & van der Lingen, 2015). Lluch-Belda et al. (1991) observed sardine (*Sardinops* sp.) peak spawning at a temperature range of 13–25°C, but spawning was constrained at intermediate values of upwelling in the California Current. In contrast, anchovy (*Engraulis* sp.) peak spawning was observed at a temperature range of 11.5–16.5°C overlapping the temperature range of sardine, but peak spawning was observed at low or high values of upwelling. The upwelling intensity seems to constrain spawning of the two species and is in line with observations of *S. pilchardus* and *S. aurita* from this study. Furthermore, the cross-shore temperature gradient, which can be interpreted as a measure of upwelling intensity, appears to be more important than temperature alone (Lluch-Belda et al., 1991), an observation also supported by our results. But increased abundances of *S. pilchardus* at SST < 18°C and of *S. aurita* at SST > 18°C still indicate spawning constrained temperature thresholds and correspond to recent observations (Ettahiri et al., 2003; Olivar, Sabatés, Pastor, & Pelegrí, 2016). Mhlongo et al. (2015) could show, although temperature regimes overlap between anchovy (*E. encrasicolus*) and sardine (*Sardinops sagax*), that both species have different preferred temperature ranges for spawning in the Benguela Current. Physiological plasticity of both species seems to

enable preferred spawning under warmer and colder conditions between years. In some years spawning of both species overlap the preferred temperature regimes, but in others the temperature regime also induces a spatio-temporal partitioning. However, relationships with upwelling may be evident during 1 year of observations, as are identified here, but given the perspective offered by decades of data in other regions, the hypothesis of spatial-temporal niche partitioning requires observations of longer duration under a wider range of ecological conditions.

Nevertheless, our results suggest, that niche partitioning has evolved due to species specific upwelling intensity preferences in the CCEBE. The partial effect of the coastal upwelling index CUI_{sst} revealed a negative correlation between larval *S. aurita* abundances and CUI_{sst} . Highest abundances were found at a CUI_{sst} of 1–5°C. This CUI_{sst} was driven by two wind components, one upwelling favorable and another southeasterly component with average speeds of 6 m s⁻¹. The optimal environmental window (OEW) hypothesis assumes a recruitment optimum at wind speeds of 5–6 m s⁻¹ in upwelling areas (Cury & Roy, 1989; Cury et al., 1995; Serra, Cury, & Roy, 1998; Waldron et al., 1997). The underlying theory of the OEW hypothesis is, that larval survival increases until wind speed reaches 5–6 m s⁻¹ inducing steady primary production, thus, food supply. In contrast, higher wind speeds cause higher mortality rates due to wind induced turbulence detrimental for larval fish feeding success (Allain, Petitgas, & Lazure, 2007; Cury & Roy, 1989; Lasker, 1981; MacKenzie, 2000). *S. aurita* larvae occurred during optimal wind conditions supporting the OEW hypothesis. However, larval *S. pilchardus* abundances were positively correlated with a CUI_{sst} of 6–7°C, which was driven by prevailing upwelling favorable wind with speeds of 7–10 m s⁻¹. According to the OEW hypothesis, these conditions seem sub-optimal for larval survival due to elevated turbulence (Roy et al., 1992).

Northeasterly trade winds, especially during the cold seasons survey 2015, transported *S. pilchardus* larvae to isobaths of more than 2,000 m, away from typical spawning grounds pre-dominantly on-shelf (Bellier, Planque, & Petitgas, 2007; Coombs et al., 2006; Ettahiri et al., 2003; John, Böhde, & Nellen, 1980; Santos et al., 2004). Ontogenetic characterization also indicated a transport of larvae from inshore to offshore for both species. Since larvae were observed within the upwelling frontal zone, the larvae must have been retained in the productive zone and were probably not affected by low food availability, due to constant nutrient input and concurrent high phytoplankton and zooplankton abundances (Sabatés & Olivar, 1996; Sánchez-Velasco, Lavín, Jiménez-Rosenberg, & Godínez, 2014). Fronts play a vital role in larval fish survival (Bakun, 2006). For instance, Munk (2014) found peak larval gadoid abundances together with peak zooplankton abundances in the vicinity of a frontal zone at the Norwegian trench. However, our observations are restricted to larval distribution patterns as far offshore as the 2,000m isobath and the upwelling front was further offshore. Therefore, it remains unresolved, whether there is a possibility for larval cross-frontal transport with a consecutive loss of larvae for recruitment.

Similar environmental conditions prevailed in both cold season surveys. *S. pilchardus* larvae were only collected in area 'A' and until 17.5°N in 2015 (Figure 3). Distribution patterns revealed an expansion of 2° latitude towards the south compared to the maximum expansion in John et al. (1980). Coombs et al. (2006) shows that spawning conditions for *S. pilchardus* are suitable along the whole permanent and seasonal upwelling area during the cold season with similar favorable temperature regimes, but in this study no larvae were found further south. It has to be conceded that our sampling periods covered 2–3 weeks, so we might have missed the whole spawning area extension. Nevertheless, although some authors believe that *S. pilchardus* populations are stationary (Ettahiri et al., 2003), others could show that *S. pilchardus* migrates far distances potentially for spawning. Some adult specimens were caught during cold years in Senegalese waters, when there was a strengthening of the trade winds (Binet, Samb, Sidi, Levenez, & Servain, 1998; Fréon, 1988).

Our observations on the highly migratory *S. aurita* indicate poleward spawning simultaneously with the influx of warm tropical water in the warm season. These results are consistent with observations of Arkhipov, Mamedov, Simanova, and Tenitskaya (2011); Arkhipov (2015) and Fréon (1988). *S. aurita* larvae also occurred infrequently in winter along the southern Senegalese area (12–15°N latitude). The temperature window, in which *S. aurita* larvae occur, comprises 18–30°C indicating a high adaptive capacity (Conand, 1977). The spawning along the southern Senegalese region in the cold season is attributed to the retentive function of the area due to a wide shelf area (Roy, 1998; Tiedemann & Brehmer, 2017). While spawning on the shelf is supposed to retain larvae onshelf, a permanent upwelling in the cold season transports nutrient rich subsurface waters providing a steady food supply for the larvae. In particular, some specimens were observed at the shelf break between 200 and 1,000m isobaths in winter 2014. That is in line with observations by Conand and Cremoux (1972), but usually the peak occurrences are inshore, where a retention cell normally retains larvae (Roy, 1998; Tiedemann & Brehmer, 2017). In the 2014 cold season, such a retention cell at the coast was absent and might explain the occurrence of some specimens further offshore.

Besides the southern Senegalese region in the cold season, another most important spawning area for *S. aurita* is the Banc d'Arguin in Mauritania in July–September (Fréon, 1988; Le Fur & Simon, 2009; Mbaye et al., 2015). Both areas are regarded as retention zones, that are supposed to be favorable for larval growth and survival (Bakun, 1996; Roy, 1998). However, our results indicate at least for the May–June period, that the Mauritanian shelf is an important spawning ground as well (Conand, 1977). The influx of warm waters along the coast, which may be representative of a decrease in coastal upwelling, is associated with the spawning of *S. aurita*. This was validated through the final GAM, that performed significantly with LFA data and the CUI_{sst} .

CUI_{sst} is a cross-shore gradient in SST, that is used as an index of coastal upwelling (Benazzouz et al., 2014) and explained more deviance of the spatially based LFA data of both species in the

GAMs than SST. The advantage using CUI_{sst} is that the temperature contrast between minimum temperatures of the upwelling and the maximum temperature offshore integrates not only SST, but also wind strength and wind direction. The temperature contrast originates from the interaction between wind field, the temperature of the subsurface upwelled water masses, and insolation (Benazzouz et al., 2014). That reduces the amount of used explanatory variables in GAMs and improves GAM performance by reducing co-linearity between explanatory variables, thus, reducing the issue of overfitting. Furthermore, the CUI_{sst} is simple to derive, inexpensive and time saving. Nevertheless, negative CUI_{sst} values, that would depict downwelling, are practically not derivable with the method they are calculated and limits the index' potential (Benazzouz et al., 2014). Flexible Tweedie distribution assumptions has improved spatial GAM modeling, which improves the handling of many zeros in count data (Miller, Burt, Rextad, & Thomas, 2013). Even with 90% zeros in the *S. aurita* LFA data, Tweedie assumption produced reliable fits of explanatory variables and provided suitable predictions of larval habitats.

Nevertheless, our limitations in the final GAMs indicate, that our sampling was not sufficient enough to explicitly generate dome-shaped relationships between LFA and explanatory variables. For instance, higher CUI_{sst} than 7°C could be negatively influencing *S. pilchardus* LFA, while CUI_{sst} of ~0 could be negatively influencing *S. aurita* LFA. Both species might reproduce on the shelf and the shelf break, but may have a limit towards offshore or inlands, although *S. pilchardus* or *S. aurita* are even found in estuaries or very close to the coast (Conand & Cremoux, 1972; Santos et al., 2004). This is also not included in the final GAM, given a sampling limit at the 20m isobaths due to ship operation constraints. Some GAM outputs are inconclusive and leave questions that will motivate future research. Do we find similar spawning patterns for other species driven by the seasonality of the upwelling? Does winds of 7–10 m s⁻¹ have a negative effect on the survival of *S. pilchardus* larvae according to the OEW hypothesis? Are larvae able to compensate strong wind events, due to a vertical migration towards deeper layers? Does the seasonality of upwelling intensity in other eastern boundary upwelling ecosystems drive similar spawning patterns of dominant small pelagic species (Lluch-Belda et al., 1991)?

Wind regimes, that are supposed to drive upwelling intensity, are anticipated to alter through climate change (Bakun et al., 2015; Rykaczewski et al., 2015). In contrast, there is an anticipated increase of temperature contrast from land to ocean enhancing trade winds and thus intensifies upwelling (Bakun, 1990; Bakun et al., 2015). A poleward displacement of upwelling-favorable winds are projected for the 21st century changing upwelling regimes in all eastern boundary ecosystems (Rykaczewski et al., 2015). Our results support the hypothesis, that larval fish habitats are shaped by species specific upwelling intensities and that changing upwelling intensity regimes can have major impacts on the expansion of larval habitats. This can explain fluctuations of dominant small pelagic species, indicating the reproductive capacity of species and future stock sizes (Rykaczewski & Checkley, 2008). Alternating upwelling intensity

regimes have been suggested to drive shifts from *S. pilchardus* dominated to *S. aurita* dominated regimes in the CCEBE (Santos, Kazmin, & Peliz, 2005; Zeeberg et al., 2008). There is a need to verify this study, not only in the CCEBE, but also in all other eastern boundary upwelling ecosystems. Such processes oriented studies can demonstrate the dependency of fish ecology to physical forces, but need *ad hoc* monitoring programs and an intensification of sampling to validate short term observations particularly in the poorly monitored southern part of the CCEBE. For instance, for the eastern boundary California Current Ecosystem (CCE) such monitoring over inter-annual and decadal exist and hydrographic models could already allow to forecast sardine production in the CCE (Rykaczewski & Checkley, 2008). For strongly exploited ecosystems like the CCEBE, monitoring campaigns are vital to estimate sustainable yields on marine resources. Thus, the development of such monitoring campaigns remains a prospective challenge. Lastly, physical models coupled with primary production are now available for the CCEBE (Auger, Gorgues, Machu, Aumont, & Brehmer, 2016) and a new model coupled with climate forecast will allow testing the effect of climate change for the fisheries sector of the CCEBE.

ACKNOWLEDGEMENTS

We thank both crews of the FRV Walther Herwig III and FRV Thalassa (AWA scientific cruise, doi:10.17600/14001400) for professional working conditions during the surveys. Luc Bonaventure Badji, Kim Wieben, Markus Simon Kraft, and Kathrin Engler are thanked for support of sampling procedures and processing of the plankton samples. Mark Taylor, Dominik Gloe, Nikolaus Probst, and Friedemann Keyl are thanked for valuable statistical recommendations. Moritz Stähler is thanked for support in R programming. This study was funded by the German Federal Ministry of Education and Research (BMBF), the Institut de Recherche pour le Développement (IRD), the Federal Research Institute for Rural Areas, Forestry and Fisheries, Thünen Institute of Sea Fisheries (TI-SF) and the Institute for Hydrobiology and Fisheries Science (IHF), as part of the tripartite project AWA (01DG12073A) 'Ecosystem Approach to the management of fisheries and the marine environment in West African waters' and the European Commission's Seventh Framework Programme (PREFACE 603521).

REFERENCES

- Allain, G., Petitgas, P., & Lazure, P. (2007). The influence of environment and spawning distribution on the survival of anchovy (*Engraulis encrasicolus*) larvae in the Bay of Biscay (NE Atlantic) investigated by biophysical simulations. *Fisheries Oceanography*, 16, 506–514.
- Alvarez-Berastegui, D., Hidalgo, M., Tugores, M. P., Reglero, P., Aparicio-González, A., Ciannelli, L., ... Alemany, F. (2016). Pelagic seascape ecology for operational fisheries oceanography: Modelling and predicting spawning distribution of Atlantic bluefin tuna in Western Mediterranean. *ICES Journal of Marine Science*, 73, 1–12.
- Aristegui, J., Barton, E. D., Alvarez-Salgado, X. A., Santos, A. M. P., Figueiras, F. G., Kifani, S., ... Demarcq, H. (2009). Sub-regional ecosystem variability in the Canary Current upwelling. *Progress in Oceanography*, 83, 33–48.
- Arkhipov, A. G. (2015). Dynamics of abundance of eggs and larvae of common fish species in the central part of the Eastern Central Atlantic. *Journal of Ichthyology*, 55, 217–223.
- Arkhipov, A. G., Mamedov, A. A., Simanova, T. A., & Tenitskaya, I. A. (2011). Dynamics of numbers of commercial fish in early ontogenesis in different areas of the Central-Eastern Atlantic. *Russian Journal of Developmental Biology*, 42, 137–142.
- Auger, P.-A., Gorgues, T., Machu, E., Aumont, O., & Brehmer, P. (2016). What drives the spatial variability of primary productivity and matter fluxes in the North-West African upwelling system? A modelling approach and box analysis. *Biogeosciences*, 13, 6419–6440.
- Augustin, N. H., Trenkel, V. M., Wood, S. N., & Lorange, P. (2013). Space-time modelling of blue ling for fisheries stock management. *Environmental Modelling*, 24, 109–119.
- Bakun, A. (1990). Global climate change and intensification of coastal ocean upwelling. *Science*, 247, 198–201.
- Bakun, A. (1996). *Patterns in the Ocean: Ocean Processes and Marine Population Dynamics*. University of California Sea Grant, California, USA, in cooperation with Centro de Investigaciones Biológicas de Noroeste, La Paz, Baja California Sur, Mexico, 323 pp.
- Bakun, A. (2006). Fronts and eddies as key structures in the habitat of marine fish larvae: Opportunity, adaptive response and competitive advantage. *Scientia Marina*, 70(Supplement 2), 105–122.
- Bakun, A., Black, B. A., Bograd, S. J., García-Reyes, M., Miller, A. J., Rykaczewski, R. R., & Sydeman, W. J. (2015). Anticipated effects of climate change on coastal upwelling ecosystems. *Current Climate Change Reports*, 1, 85–93.
- Beale, C. M., Lennon, J. J., Yearsley, J. M., Brewer, M. J., & Elston, D. A. (2010). Regression analysis of spatial data. *Ecology Letters*, 13, 246–264.
- Bellier, E., Planque, B., & Petitgas, P. (2007). Historical fluctuations in spawning location of anchovy (*Engraulis encrasicolus*) and sardine (*Sardina pilchardus*) in the Bay of Biscay during 1967–73 and 2000–2004. *Fisheries Oceanography*, 16, 1–15.
- Benazzouz, A., Mordane, S., Orbi, A., Chagdali, M., Hilmi, K., Atillah, A., ... Demarcq, H. (2014). An improved coastal upwelling index from sea surface temperature using satellite-based approach - The case of the Canary Current upwelling system. *Continental Shelf Research*, 81, 38–54.
- Binet, D., Samb, B., Sidi, M.T., Levenez, J.-J., & Servain, J. (1998). Sardine and other pelagic fisheries changes associated with multi-year trade wind increases in the Southern Canary Current. In M.-H. Durand, P. Cury, R. Mendelssohn, C. Roy, A. Bakun & D. Pauly (Eds.), *Global versus local changes in upwelling systems* (pp. 211–233). Paris: ORSTOM.
- Botsford, L. W., Lawrence, C. A., Dever, E. P., Hastings, A., & Largier, J. (2003). Wind strength and biological productivity in upwelling systems: An idealized study. *Fisheries Oceanography*, 12, 245–259.
- Braham, C.-B., & Corten, A. (2015). Pelagic fish stocks and their response to fisheries and environmental variation in the Canary Current large marine ecosystem. In L. Valdés & I. Déniz-González (Eds.), *Oceanographic and biological features in the Canary Current large marine ecosystem* (pp. 196–214). Paris: UNESCO.
- Braham, C.-B., Fréon, P., Laurec, A., Demarcq, H., & Bez, N. (2014). New insights in the spatial dynamics of sardinella stocks off Mauritania (North-West Africa) based on logbook data analysis. *Fisheries Research*, 154, 195–204.
- Conand, F. (1977). Oeufs et larves de la sardinelle ronde (*Sardinella aurita*) au Sénégal: Distribution, croissance mortalité, variations d'abondance de 1971 à 1976. *Cahiers ORSTOM. Série Océanographie*, 15, 201–214.
- Conand, F. (1978). Systématique des larves de clupéidés de l'Atlantique orientale entre 20°N et 15°S (eaux marines et saumâtres). *Cahiers ORSTOM. Série Océanographie*, 16, 3–8.
- Conand, F., & Cremoux, J.L. (1972). *Distribution et abondance des larves de sardinelles dans la région du Cap - Vert de septembre 1970 à août 1971*. Dakar-Thiaroye: ORSTOM, FAO, DSP no 36, 33 pp.

- Coombs, S. H., Smyth, T. J., Conway, D. V. P., Halliday, N. C., Bernal, M., Stratoudakis, Y., & Alvarez, P. (2006). Spawning season and temperature relationships for sardine (*Sardina pilchardus*) in the eastern North Atlantic. *Journal of the Marine Biological Association of the United Kingdom*, 86, 1245–1252.
- Craney, T. A., & Surlis, J. G. (2002). Model-dependent variance inflation factor cutoff values. *Quality Engineering*, 14, 391–403.
- Cropper, T. E., Hanna, E., & Bigg, G. R. (2014). Spatial and temporal seasonal trends in coastal upwelling off Northwest Africa, 1981–2012. *Deep Sea Research Part I: Oceanographic Research Papers*, 86, 94–111.
- Cury, P., & Roy, C. (1989). Optimal environmental window and pelagic fish recruitment success in upwelling areas. *Canadian Journal of Fisheries and Aquatic Science*, 46, 670–680.
- Cury, P., Roy, C., Mendelsohn, R., Bakun, A., Husby, D. M., & Parrish, R. H. (1995). Moderate is better: Exploring nonlinear climatic effects on the Californian northern anchovy (*Engraulis mordax*). *Canadian Special Publication of Fisheries and Aquatic Sciences*, 121, 417–424.
- Ditty, J. G., Houde, E. D., & Shaw, R. F. (1994). Egg and larval development of sardine *Sardinella aurita* (Family Clupeidae) with a synopsis of characters to identify clupeid larvae from the northern Gulf of Mexico. *Bulletin of Marine Science*, 54, 367–380.
- Doi, T., Tozuka, T., & Yamagata, T. (2009). Interannual variability of the Guinea Dome and its possible link with the Atlantic Meridional Mode. *Climate Dynamics*, 33, 985–998.
- Ekman, W. V. (1905). On the influence of the earth's rotation on ocean currents. *Arkiv för matematik, astronomi och fysik*, 2, 1–51.
- Ettahiri, O., Berraho, A., Vidy, G., Ramdani, M., & Do chi, T. (2003). Observation on the spawning of sardina and sardinella off the south Moroccan Atlantic coast (21–26°N). *Fisheries Research*, 60, 207–222.
- Fahrig, L. (1992). Relative importance of spatial and temporal scales in a patchy environment. *Theoretical Population Biology*, 41, 300–314.
- Faye, S., Lazar, A., Sow, B. A., & Gaye, A. T. (2015). A model study of the seasonality of sea surface temperature and circulation in the Atlantic North-eastern tropical upwelling system. *Frontiers in Physics*, 3, 1–20.
- Fréon, P. (1988). Responses et adaptations des stocks de cupleides d'Afrique de l'ouest à la variabilité du milieu et de l'exploitation. *L'Université d'Aix Marseille*, 287 pp.
- Gittleman, J. L., & Kot, M. (1990). Adaptation: Statistics and a null model for estimating phylogenetic effects. *Systematic Zoology*, 39, 227–241.
- Gushchin, A. V., & Corten, A. (2015). Feeding of pelagic fish in waters of Mauritania: 1. European anchovy *Engraulis encrasicolus*, European sardine *Sardina pilchardus*, round sardinella *Sardinella aurita*, and flat sardinella *S. maderensis*. *Journal of Ichthyology*, 55, 77–85.
- Hastie, T., & Tibshirani, R. (1986). Generalized additive models. *Statistical Science*, 1, 297–318.
- ter Hofstede, R., & Dickey-Collas, M. (2006). An investigation of seasonal and annual catches and discards of the Dutch pelagic freezer-trawlers in Mauritania, Northwest Africa. *Fisheries Research*, 77, 184–191.
- Johannes, R. E. (1978). Reproductive strategies of coastal marine fishes in the tropics. *Environmental Biology of Fishes*, 3, 65–84.
- John, H.-C., Böhde, U. J., & Nellen, W. (1980). *Sardina pilchardus* larvae in their southernmost range. *Archiv für Fischereiwissenschaft*, 31, 67–85.
- JPOurOceanProject. (2010). GHRSSST Level 4 G1SST global foundation sea surface temperature analysis. Ver. 1. PO.DAAC, CA, USA. Dataset accessed [2015-09-23] at Retrieved from <https://doi.org/10.5067/ghg1s-4fp01>
- KNMI. (2010) MetOp-A ASCAT Level 2 Ocean surface wind vectors optimized for coastal ocean. Ver. Operational/Near-Real-Time. PO.DAAC, CA, USA. Dataset accessed [2015-09-23].
- Lasker, R. (1981). The role of a stable ocean in larval fish survival and subsequent recruitment. In R. Lasker (Ed.), *Marine fish larvae: Morphology, ecology and relation to fisheries* (pp. 80–87). Seattle: University Washington Press.
- Le Fur, J., & Simon, P. (2009). A new hypothesis concerning the nature of small pelagic fish clusters An individual-based modelling study of *Sardinella aurita* dynamics off West Africa. *Ecological Modelling*, 220, 1291–1304.
- León-Chávez, C. A., Beier, E., Sánchez-Velasco, L., Barton, E. D., & Godínez, V. M. (2015). Role of circulation scales and water mass distributions on larval fish habitats in the eastern tropical pacific off Mexico. *Journal of Geophysical Research*, 120, 3987–4002.
- Lluch-Belda, D., Lluch-Cota, D.B., Hernandez-Vazquez, S., Salinas-Zavala, C.A., & Schwartzlose, R.A. (1991). Sardine and anchovy spawning as related to temperature and upwelling in the California current system. *CALCOFI Reports*, 32, 7 pp.
- Machu, E., Ettahiri, O., Kifani, S., Benazzouz, A., Makaoui, A., & Demarcq, H. (2009). Environmental control of the recruitment of sardines (*Sardina pilchardus*) over the western Saharan shelf between 1995 and 2002: A coupled physical/biochemical modelling experiment. *Fisheries Oceanography*, 18, 287–300.
- MacKenzie, B. R. (2000). Turbulence, larval fish ecology and fisheries recruitment: A review of field studies. *Oceanologica Acta*, 23, 357–375.
- Mbaye, B. C., Brochier, T., Echevin, V., Alban, L., Levy, M., Mason, E., ... Machu, E. (2015). Do *Sardinella aurita* spawning seasons match local retention patterns in the Senegalese – Mauritanian upwelling region? *Fisheries Oceanography*, 24, 69–89.
- Mgurk, M. D. (1986). Natural mortality of marine pelagic fish eggs and larvae: Role of spatial patchiness. *Marine Ecology Progress Series*, 34, 227–242.
- Mhlongo, N., Yemane, D., Hendricks, M., & van der Lingen, C. D. (2015). Have the spawning habitat preferences of anchovy (*Engraulis encrasicolus*) and sardine (*Sardinops sagax*) in the southern Benguela changed in recent years? *Fisheries Oceanography*, 24, 1–14.
- Miller, D. L., Burt, M. L., Rexstad, E. A., & Thomas, L. (2013). Spatial models for distance sampling data: Recent developments and future directions. *Methods in Ecology and Evolution*, 4, 1001–1010.
- Mittelstaedt, E. (1991). The ocean boundary along the northwest African coast: Circulation and oceanographic properties at the sea surface. *Progress in Oceanography*, 26, 307–355.
- Munk, P. (2014). Fish larvae at fronts: Horizontal and vertical distributions of gadoid fish larvae across a frontal zone at the Norwegian Trench. *Deep Sea Research Part II: Topical Studies in Oceanography*, 107, 3–14.
- Murray, L., Nguyen, H., Lee, Y.-F., Remmenga, M.D., & Smith, D.W. (2012). Variance inflation factors in regression models with dummy variables. *Annual conference on applied statistics in agriculture*, 12: 161–177.
- Olivar, M. P., Sabatés, A., Pastor, M. V., & Pelegrí, J. L. (2016). Water masses and mesoscale control on latitudinal and cross-shelf variations in larval fish assemblages off NW Africa. *Deep Sea Research Part I: Oceanographic Research Papers*, 117, 120–137.
- Pastor, M. V., Pelegrí, J. L., Hernández-Guerra, A., Font, J., Salat, J., & Emelianov, M. (2008). Water and nutrient fluxes off Northwest Africa. *Continental Shelf Research*, 28, 915–936.
- Pebesma, E. J. (2004). Multivariable geostatistics in S: The gstat package. *Computers & Geosciences*, 30, 683–691.
- Pollard, R. T., Rhines, P. B., & Thompson, R. O. R. Y. (1973). The deepening of the wind-mixed layer. *Geophysical & Astrophysical Fluid Dynamics*, 4, 381–404.
- Pringle, J. M. (2007). Turbulence avoidance and the wind-driven transport of plankton in the surface Ekman layer. *Continental Shelf Research*, 27, 670–678.
- Ré, P., & Meneses, I. (2008). *Early stages of marine fishes occurring in the Iberian Peninsula*. IPIMAR/IMAR, 282 pp.
- Rooker, J. R., Simms, J. R., Wells, R. J. D., Holt, S. A., Holt, G. J., Graves, J. E., & Furey, N. B. (2012). Distribution and habitat associations of

- billfish and swordfish larvae across mesoscale features in the Gulf of Mexico. *PLoS One*, 7, 1–14.
- Roy, C. (1998). An upwelling-induced retention area off Senegal: A mechanism to link upwelling and retention processes. *South African Journal of Marine Science*, 19, 89–98.
- Roy, C., Cury, P., Fréon, P., & Demarcq, H. (2002). Environmental and resource variability off Northwest Africa and in the Gulf of Guinea: A review. In J. M. McGlade, P. Cury, K. A. Koranteng & N. J. Hardman-Mountford (Eds.), *The Gulf of Guinea large marine ecosystem* (pp. 121–139). Elsevier, Amsterdam.
- Roy, C., Cury, P., & Kifani, S. (1992). Pelagic fish recruitment success and reproductive strategy in upwelling areas: Environmental compromises. *South African Journal of Marine Science*, 12, 135–146.
- Russell, F.S. (1976). *The eggs and planktonic stages of British marine fishes*. London-New York-San Francisco: Academic Press, 524 pp.
- Rykaczewski, R. R., & Checkley, D. M. (2008). Influence of ocean winds on the pelagic ecosystem in upwelling regions. *Proceedings of the National Academy of Sciences of the United States of America*, 105, 1965–1970.
- Rykaczewski, R. R., Dunne, J. P., Sydeman, W. J., García-Reyes, M., Black, B. A., & Bograd, S. J. (2015). Poleward displacement of coastal upwelling-favorable winds in the ocean's eastern boundary currents through the 21st century. *Geophysical Research Letters*, 42, 6424–6431.
- Sabatés, A., & Olivar, M. P. (1996). Variation of larval fish distributions associated with variability in the location of a shelf-slope front. *Marine Ecology Progress Series*, 135, 11–20.
- Sánchez-Velasco, L., Lavín, M. F., Jiménez-Rosenberg, S. P. A., & Godínez, V. M. (2014). Preferred larval fish habitat in a frontal zone of the northern Gulf of California during the early cyclonic phase of the seasonal circulation (June 2008). *Journal of Marine Systems*, 129, 368–380.
- Santos, A. M. P., de Fátima Borges, M., & Groom, S. (2001). Sardine and horse mackerel recruitment and upwelling off Portugal. *ICES Journal of Marine Science*, 58, 589–596.
- Santos, A. M. P., Kazmin, A. S., & Peliz, Á. (2005). Decadal changes in the Canary upwelling system as revealed by satellite observations: Their impact in the productivity. *Journal of Marine Research*, 63, 359–379.
- Santos, A. M. P., Peliz, A., Dubert, J., Oliveira, P. B., Angélico, M. M., & Ré, P. (2004). Impact of a winter upwelling event on the distribution and transport of sardine (*Sardina pilchardus*) eggs and larvae off western Iberia: A retention mechanism. *Continental Shelf Research*, 24, 149–165.
- Schoener, T. W. (1974). Resource partitioning in ecological communities. *Science*, 185, 27–39.
- Serra, R., Cury, P., & Roy, C. (1998). The recruitment of the Chilean sardine (*Sardinops sagax*) and the "optimal environmental window". In M. Durand, P. Cury, R. Mendelssohn, C. Roy, A. Bakun, & D. Pauly (Eds.), *Global versus local changes in upwelling systems* (pp. 267–274). Monterey, CA: ORSTOM.
- Shono, H. (2008). Application of the Tweedie distribution to zero-catch data in CPUE analysis. *Fisheries Research*, 93, 154–162.
- Smith, P.E., & Richardson, S.L. (1977). Standard techniques for pelagic fish egg and larval surveys. Admin. Report No. LJ-77-11. 108 pp.
- Tiedemann, M., & Brehmer, P. (2017). Larval fish assemblages across an upwelling front: Indication for active and passive retention. *Estuarine, Coastal and Shelf Science*, 187C, 118–133.
- Tomczak, M. (1981). An analysis of mixing in the frontal zone of South and North Atlantic Central Water off North - West Africa. *Progress in Oceanography*, 10, 173–192.
- Tsikliras, A. C. (2014). Sympatric clupeoid fish larvae in the Northeastern Mediterranean: Coexistence or avoidance? *Advances in Ecology*, 2014, 1–8.
- Van Camp, L., Nykjaer, L., Mittelstaedt, E., & Schlittenhardt, P. (1991). Upwelling and boundary circulation off Northwest Africa as depicted by infrared and visible satellite observations. *Progress in Oceanography*, 26, 357–402.
- Waldron, H. N., Brundri, G. B., & Probyn, T. A. (1997). Anchovy biomass is linked to annual potential new production in the southern Benguela: Support for the "optimal environmental window" hypothesis. *South African Journal of Marine Science*, 18, 107–112.
- Wang, Y. T., & Tzeng, W. N. (1997). Temporal succession and spatial segregation of clupeoid larvae in the coastal waters off the Tanshui River Estuary, northern Taiwan. *Marine Biology*, 129, 23–32.
- Welch, B. L. (1951). On the comparison of several mean values: An alternative approach. *Biometrika*, 38, 330–336.
- Winton, M., Wuenschel, M., & McBride, R. (2014). Investigating spatial variation and temperature effects on maturity of female winter flounder (*Pseudopleuronectes americanus*) using generalized additive models. *Canadian Journal of Fisheries and Aquatic Science*, 71, 1279–1290.
- Wood, S. N. (2003). Thin-plate regression splines. *Journal of the Royal Statistical Society: Series B (Statistical Methodology)*, 65, 95–114.
- Wood, S. N. (2006). *Generalized additive models: An introduction with R* (p. 392). Boca Raton, FL: Taylor & Francis Group.
- Wooster, W. S., Bakun, A., & McLain, D. R. (1976). The seasonal upwelling cycle along the eastern boundary of the North Atlantic. *Journal of Marine Research*, 34, 131–141.
- Zeeberg, J., Corten, A., Tjoe-Awie, P., Coca, J., & Hamady, B. (2008). Climate modulates the effects of *Sardinella aurita* fisheries off Northwest Africa. *Fisheries Research*, 89, 65–75.
- Zenk, W., Klein, B., & Schroder, M. (1991). Cape Verde frontal zone. *Deep Sea Research Part I: Oceanographic Research Papers*, 38, 505–530.
- Zuur, A. F., Ieno, E. N., & Elphick, C. S. (2010). A protocol for data exploration to avoid common statistical problems. *Methods in Ecology and Evolution*, 1, 3–14.

SUPPORTING INFORMATION

Additional Supporting Information may be found online in the supporting information tab for this article.

How to cite this article: Tiedemann M, Fock HO, Brehmer P, Döring J, Möllmann C. Does upwelling intensity determine larval fish habitats in upwelling ecosystems? The case of Senegal and Mauritania. *Fish Oceanogr.* 2017;26:655–667. <https://doi.org/10.1111/fog.12224>